Figure S1. Altered miR-922 expression changes malignant behavior of liver cancer cells. (A) Cell Counting Kit-8 tested proliferation of each group of MHCC97L cells. (Bi and Bii) Flow cytometry analyzed the number of apoptotic MHCC97L cells in each group. (Ci and Cii) Transwell invasion assays detected MHCC97L cell invasion ability. (Di and Dii) Colony formation assay determined clonogenicity of each group of MHCC97L cells. (Ei and Eii) Wound healing assays assessed the migration ability of MHCC97L cells. **P<0.01, ***P<0.001, ****P<0.0001. miR, microRNA; OD, optical density.

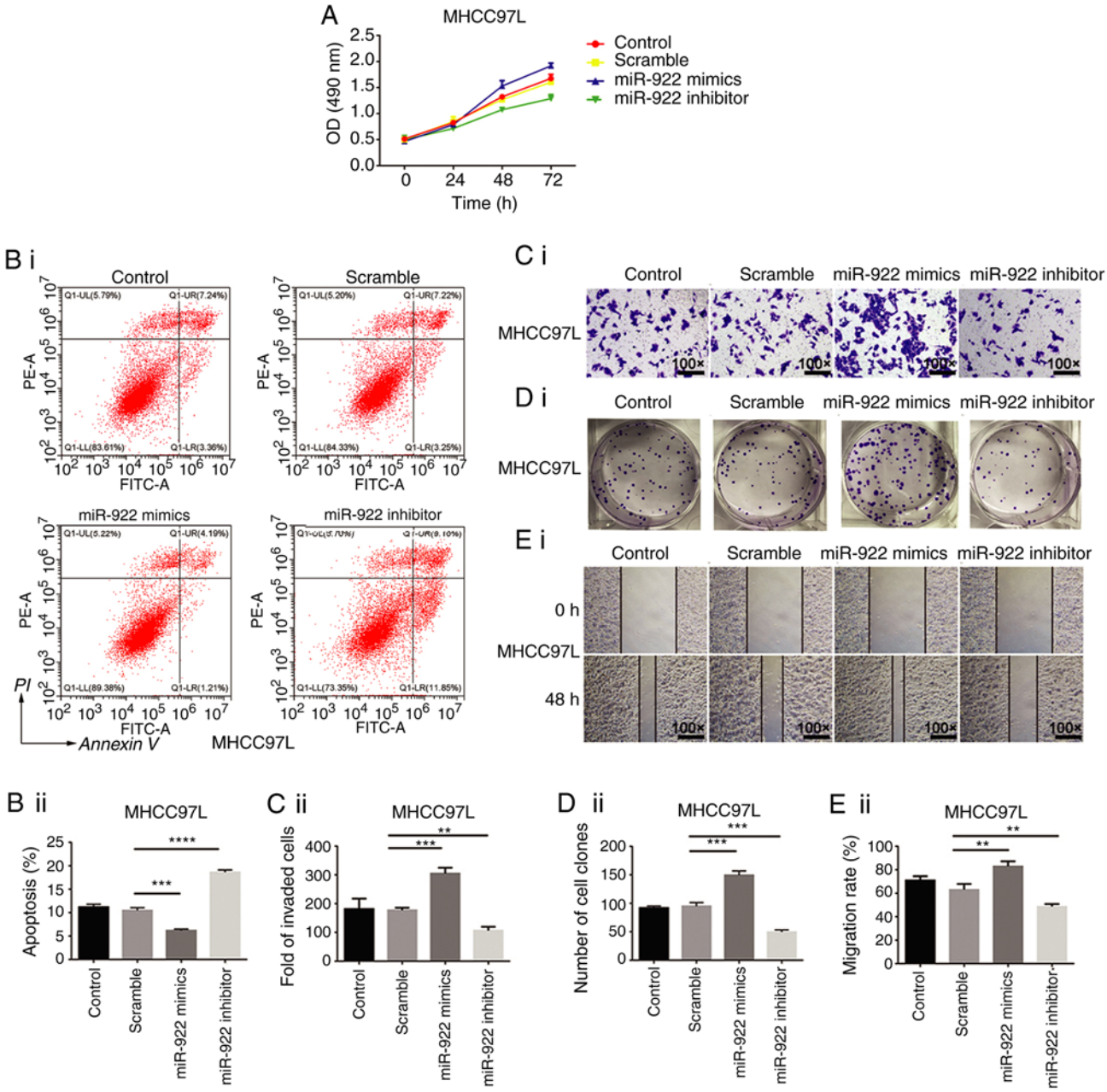

Figure S2. Altered *ARID2* expression changes malignant behavior of MHCC97L cells *in vitro*. The proliferation, clonogenicity, apoptosis, wound healing and invasion of MHCC97L cells were determined following altered *ARID2* expression. (A) Cell Counting Kit-8 assay determined cell proliferation. (Bi and Bii) Flow cytometry of apoptotic MHCC97L cells. (Ci and Cii) Cell clonogenicity of MHCC97L cells. (Di and Dii) Transwell assay analysis of MHCC97L cell invasion. (Ei and Eii) Wound healing analysis of MHCC97L cell proliferation and migration. Data are presented as the mean ± SD (n=3). *P<0.05, ***P<0.001. *ARID2*, *ARID2*, AT-rich interactive domain 2; OD, optical density; NC, negative control; sh, short hairpin; OE, overexpression.

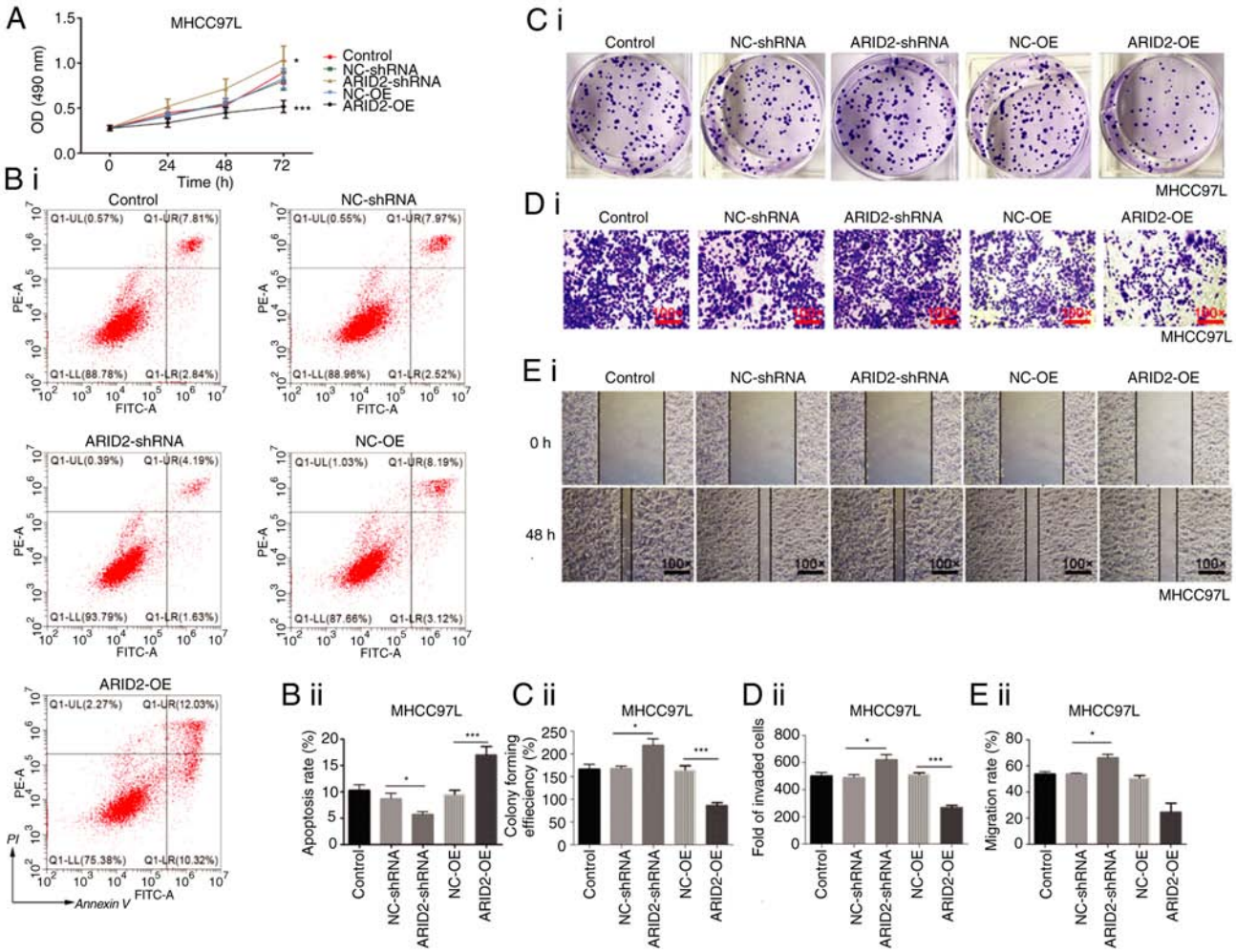

Figure S3. Altered *ARID2* expression modulates expression levels of Bax, Bcl-2, *MMP3* and *MMP9*. Expression levels of Bax, Bcl-2, *MMP3* and *MMP9* in tumor tissue were assessed by immunohistochemistry. *ARID2*, *ARID2*, AT-rich interactive domain 2; CON, control; NC, negative control; sh, short hairpin; OE, over-expression.

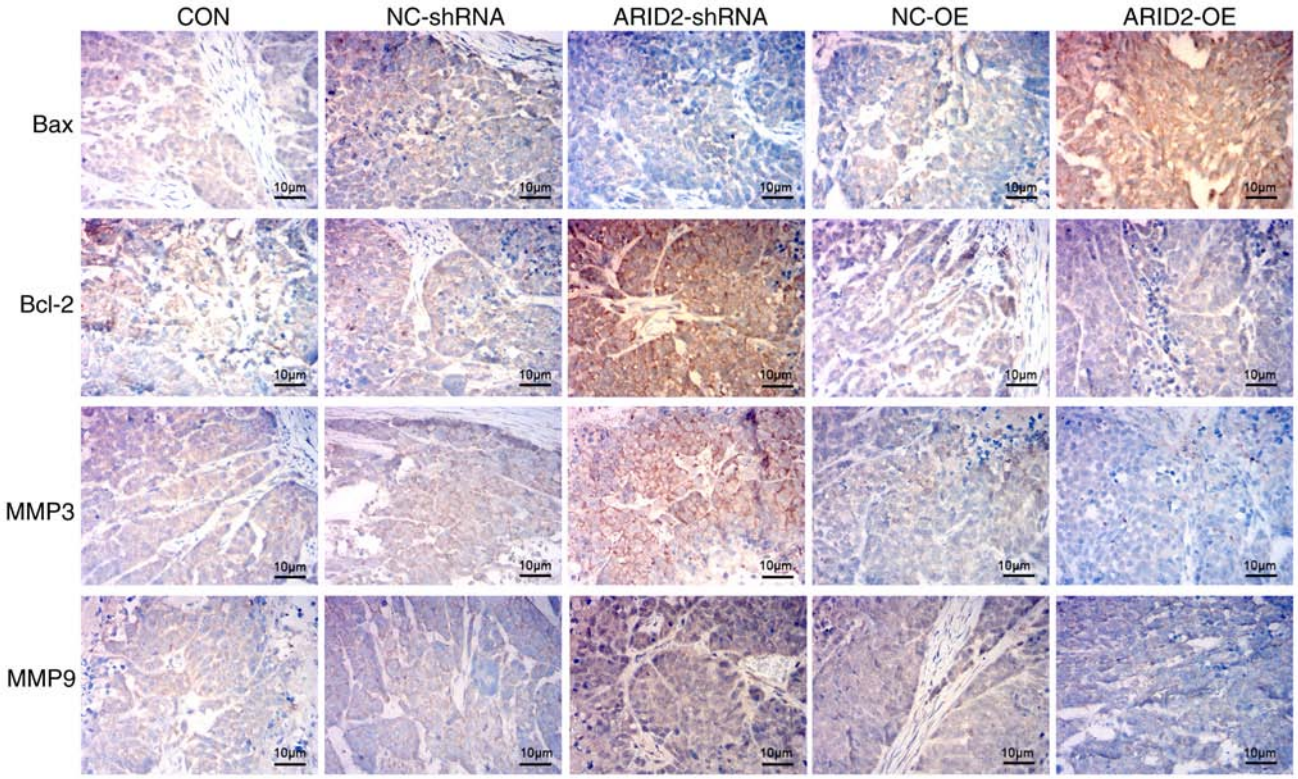

Figure S4. Altered *ARID2* expression modulates miR-922 inhibitor-decreased malignant behavior of MHCC97L cells. MHCC97L cells were stably transfected with miR-922 inhibitor and transfected with plasmid for *ARID2* expression or *ARID2*-specific shRNA for *ARID2* silencing. Control cells were transfected with vehicles. (A) Cell Counting Kit-8 determined proliferation of MHCC97L cells. (Bi and Bii) Number of apoptotic MHCC97L cells was analyzed by flow cytometry. (Ci and Cii) Clonogenicity was analyzed by colony formation assay. (Di and Dii) Transwell assay analysis of invasion of each group of cells. (Ei and Eii) Wound healing analysis of each group of MHCC97L cells. Data are presented as the mean ± SD (n=3). *P<0.05, **P<0.01, ***P<0.001 ****P<0.0001. *ARID2*, *ARID2*, AT-rich interactive domain 2; miR, microRNA; sh, short hairpin; OD, optical density, OE, over-expression; NC, negative control.

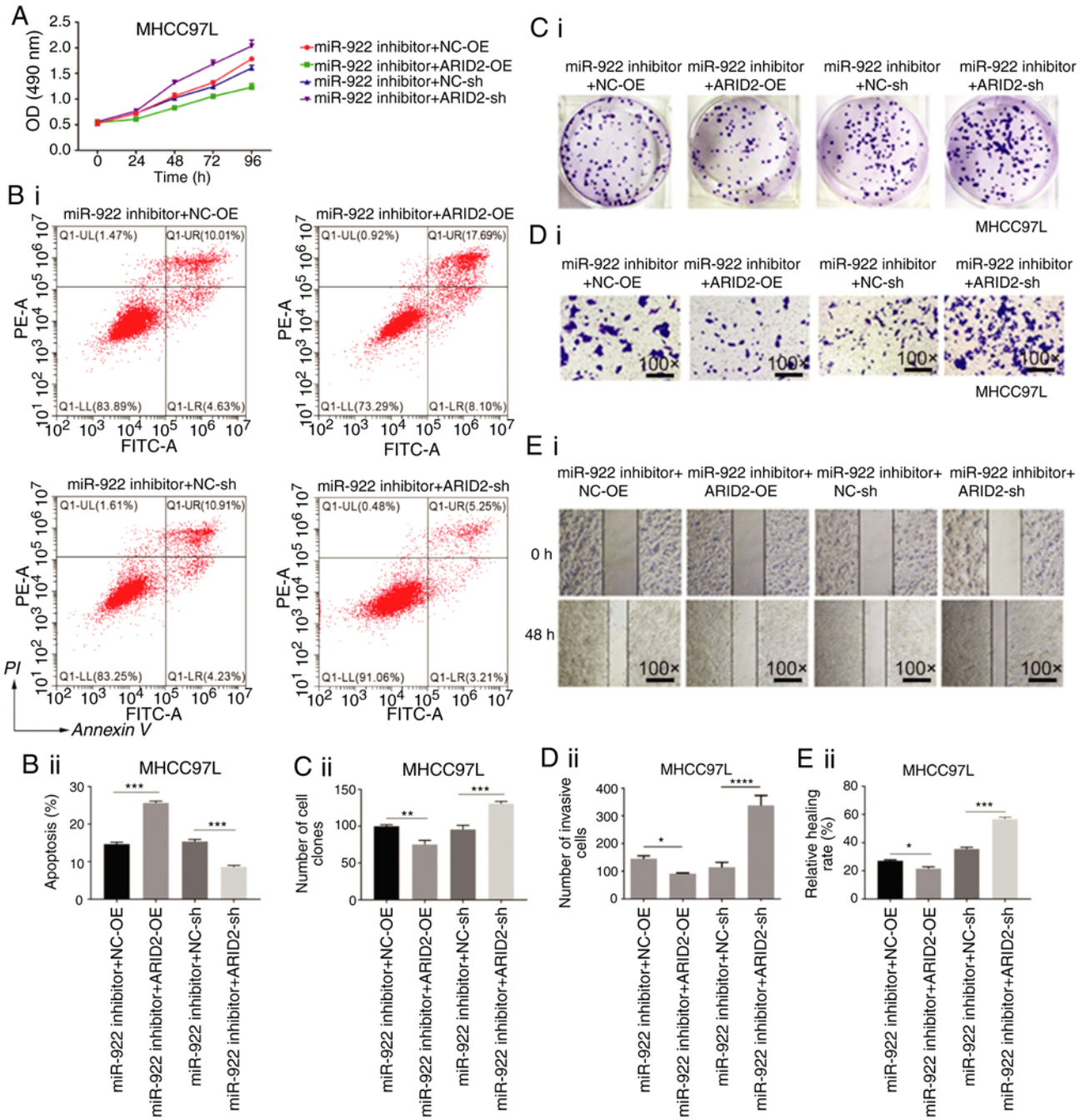

Figure S5. Reverse transcription-quantitative PCR analysis of levels of miR-922 mimics and inhibitor transcripts after transfection of HepG2 and MHCC97L cells, respectively. Data are presented as the mean ± SD (n=3). **P<0.01, ***P<0.001. NC, negative control.

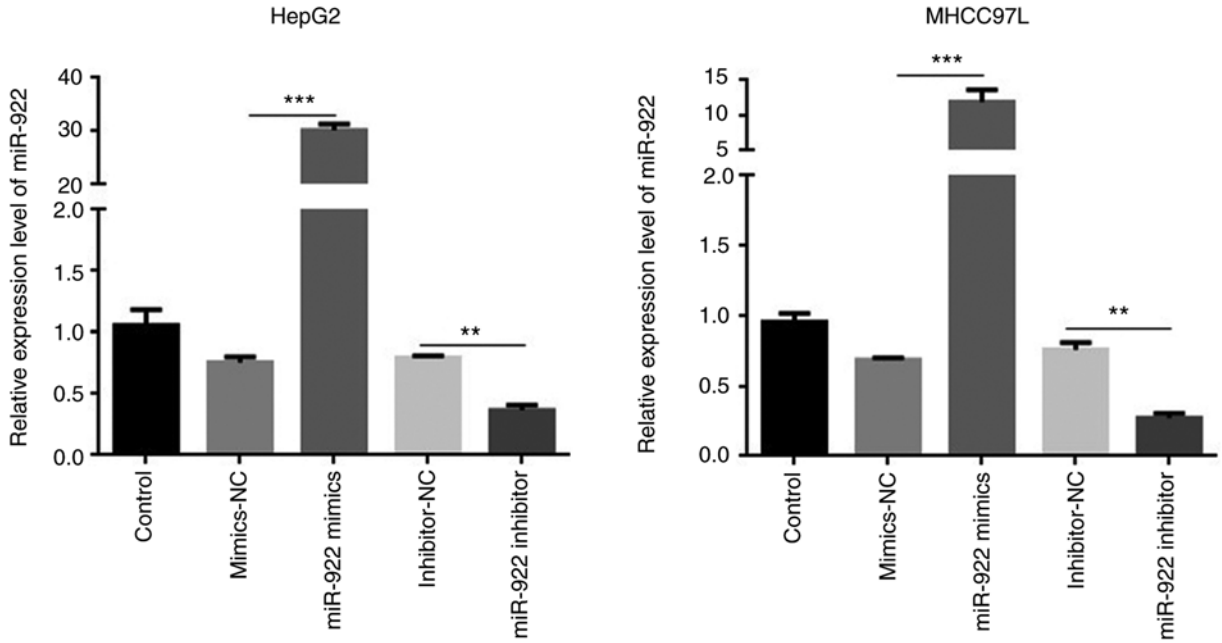

Figure S6. *ARID2* cDNA was cloned into the plasmid pcDNA3.1 to establish the *ARID2* overexpression plasmid, which was transfected into HEK293 cells. DNA fragments for expression of three *ARID2* interference shRNAs or sh-NC sequence were designed and cloned into the pGPU6 plasmid. Subsequently, the established plasmids were transfected into HEK293 cells to validate *ARID2* over-expression and the inhibitory effects of *ARID2*-specific shRNA on *ARID2* expression by western blotting. Data are presented as the mean ± SD (n=3). ***P<0.001. miR, microRNA; *ARID2*, AT-rich interactive domain 2; sh, short hairpin; NC, negative control; OE, over-expression; ns, not significant.